

**Of sequence and structure: Strategies of protein thermostability in evolutionary perspective**

Igor N. Berezovsky and Eugene I. Shakhnovich\*

Department of Chemistry and Chemical Biology, Harvard University, 12 Oxford Street, Cambridge, MA 02138

\*Correspondence should be directed to Prof. Eugene I. Shakhnovich, Department of Chemistry and Chemical Biology, Harvard University, 12 Oxford Street, Cambridge, MA 02138, phone: 617-495-4130, fax: 617-384-9228, e-mail: [eugene@belok.harvard.edu](mailto:eugene@belok.harvard.edu)

Biological sciences: Biophysics, Evolution

## **Abstract**

Although discussions about the mechanisms and major contributors to the thermostability of proteins have been ongoing for several decades, there are not, as of yet, any general rules describing the phenomenon. Here, we have started from the consideration of general concepts of thermostability, which leads us to hypotheses about structure-based and sequence-based mechanisms. Our simulations confirmed the idea that there are two major strategies of protein thermostability: (i) general, non-specific, structure-based, with contribution from all types of stabilizing interactions, and (ii) specific, sequence-based, with use of only dominating factor for adaptation to extreme conditions. The choice of a certain strategy is a direct consequence of the need to balance the demands of environmental conditions and the diversity of the proteomes of respective species at different stages of evolution. The existence of two strategies of thermostability gives us insight into the role of particular interactions and ways of designing proteins with desired stabilities.

## Introduction

The importance of different factors contributing to protein thermostability remains a subject of intense study (1-7). The most frequently reported trends include increased van der Waals interactions (8), higher core hydrophobicity (9), additional networks of hydrogen bonds (7), enhanced secondary structure propensity (10), ionic interactions (11), increased packing density (12), and decreased length of surface loops (13).

Recently, it was demonstrated that proteins use various combinations of these mechanisms (11, 14, 15). However, no general rule for increasing thermostability (2, 16) was found. The diversity of the “recipes” for thermostability immediately raises two important questions: (i) is there a common evolutionary or physical basis for these apparently different mechanisms, and (ii) how did this diversity of mechanisms appear and develop on the evolutionary scene?

To address the first question, one has to go beyond the analysis of specific stabilizing interactions and their various combinations. Conceptually, then, there can be two major factors that affect protein thermostability. First, thermostable proteins may have structural bias such as enhanced packing. Second, particular substitutions made in sequences of mesophilic proteins can provide formation of “staples”, i.e. specific and strong interactions without significantly altering protein structure. We, therefore, posit two apparent foundations for protein thermostability, *structure and sequence*, each having their own advantages and drawbacks. Structure-based thermostability is *non-specific* in the sense that no or minimal special features of sequences are needed to achieve thermostability, making it robust under a wide range of environmental conditions. A possible evolutionary disadvantage of such a robust stabilization

mechanism is that it makes the protein less adaptable to rapid and specific changes in environmental conditions. In contrast, just a few strategic substitutions in sequence can lead to significant stabilization of an existing structure through the formation of several strong interactions *specific* to certain demands of the environment. These “staples” can work locally, leaving the bulk of the structure and its compactness unchanged. There is, however, also a possible disadvantage to this mechanism. Sequence-based stabilization may not be robust because it is typically tailored to a specific and narrow range of environmental conditions.

The last but not least, there may be an additional crucial factor affecting the choice between specific, sequence-based, versus non-specific, structure-based, stabilization mechanism - availability of the sequence/structure repertoire at different stages of protein evolution. At the beginning of protein evolution, only a restricted number of primordial structures/sequences were available and mutation/modification machinery was not yet fully developed. Thus, selection towards more thermostable proteins could happen only on the basis of utilizing existing and relatively simple structures. This factor made *non-specific*, structure-based mechanisms most probable and reliable way of gaining increased stability. Later on, when diversity of sequences became wide enough, the search in sequence space appeared to be another important mechanism for *specific* modification of the structure. While evolution of protein structure most likely started with structure-based mechanism(s) of thermostability, sequence-related ones eventually became important contributors by effective mutation processes under different environmental conditions. Finally, “long-time” evolutionary experiments endowed variety of the recipes to the vast diversity of biological material. All the evolutionary

scenarios leading to a particular strategy comprised what we will term the “evolutionary basis” for that strategy.

In this work we demonstrate the existence of two strategies for achieving protein thermostability, structure-based and sequence-based, and show that selection of a particular strategy for thermal adaptation can be understood in evolutionary context.

## **Materials and methods**

The set of proteins we have analyzed in this work consists of 5 groups: 1. Hydrolase, from *E.coli* (1INO) and *T. thermophilus* (2PRD); 2. Rubredoxin, from *D. gigas* (1RDG), *C. pasteurianum* (5RXN), *D. vulgaris* (8RXN), and *P. furiosus* (1CAA); 3. 2Fe-2S Ferredoxin, from *S. platensis* (4FXC), *E. arvensis* (1FRR), *Anabaena PCC7120* (1FRD), *H. marismortui* (1DOI), and *S. elongatus* (2CJN); 4. 4Fe-4S Ferredoxin, from *C. acidurici* (1FCA), *P. asaccharolyticus* (1DUR), *B. thermoproteolyticus* (1IQZ), and *T. maritima* (1VJW); 5. Chemotaxis protein, from *E. coli* (3CHY), *S. typhimurium* (2CHF), and *T. maritima* (1TMY). X-ray data from the Protein Data Bank were supplemented with coordinates of H-atoms (16) .

Unfolding simulations were performed using an all-atom Go model developed earlier (17). In the Go interaction scheme atoms that are neighbors in the native structure are assumed to have attractive interactions. Hence Go model of interactions is structure-based. Every unfolding run consists of  $2 \times 10^6$  steps. The move set contains one backbone move followed by one side-chain move. Van der Waals interactions were calculated for atoms belonging to residues separated by at least two residues along the polypeptide chain; only contact distances within 2.5-5.0 Å were considered for interactions (16).

High-throughput analyzes of the distributions of van der Waals contacts was performed on representative sets of major fold types, all  $\alpha$ , all  $\beta$ ,  $\alpha/\beta$ ,  $\alpha+\beta$  (according to SCOP classification (18), for list of the proteins used in the analysis see Supporting Information), from *T. maritima*, *P. Furiosis/Horikoshii/Abyssi*, and *T. thermophilus*. Jack-knife tests have been performed to exclude: (i) possible effect of the same fold on the set, and (ii) influence of the size of the set.

Numbers of rotamers in fully unfolded states of Hydrolases (1INO and 2PRD) were calculated. Structures were unfolded at high temperature  $T=4$  (see Figure 1A). Coordinate snapshots were recorded at every  $10^5$  steps MC steps of total  $10^7$  steps done for every structure. Numbers of rotamers for every residue were determined as an average over 100 snapshot.

Hydrogen bonds were determined according to criteria developed in (19, 20).

Sequence alignments were done using software “MultAlign” developed in (21).

## Results

The aims of our analysis were twofold: (i) to outline major strategies of protein thermostability, and (ii) to find an evolutionary basis for the development of particular strategies in the variety of species. These considerations defined the choice of the set of analyzed proteins. It includes five groups of proteins, each of them containing representatives of mesophilic organisms and its analogues from (hyper)thermophilic species. At the same time, members of these groups represent evolutionarily distant branches of the phylogenetic tree, archaea and bacteria. First, we evaluated stability of each of the proteins using an unfolding procedure based on the Go model (22).

According to the Go model native interactions in the structure of the natural protein reflect mutually stabilizing effects of all or almost all types of interactions. Thus Go-model simulations aim at revealing *structure-based* contributions to protein stability. Unfolding simulation for the studied groups of proteins reveal general trends of higher transition temperatures of unfolding for several (hyper)thermophilic proteins compared to their mesophilic counterparts. Figure 1A shows the difference between the hydrolases from thermophilic *T. thermophilus* and mesophilic *E.coli* towards higher stability of thermophilic protein. There is a pronounced difference between the unfolding temperatures of the rubredoxin from hyperthermophilic *P. furiosus* and rubredoxins from three mesophilic organisms (Figure 1B). Three mesophilic 2Fe-2S ferredoxins (4FXC, 1FRR, and 1FRD) demonstrate a narrow range of transition temperatures, whereas the thermophilic one (2CJN) from cyanobacterium *S. elongatus* has a substantially higher temperature of unfolding (Figure 1C). Analysis of 4Fe-4S ferredoxins from mesophilic and thermophilic organisms also reveals a significant difference in their transition temperatures (Figure 1D) demonstrating increased thermostability of thermophilic ferredoxin (1IQZ).

A striking exception from the general rule of higher simulation transition temperature for (hyper)thermostable proteins is demonstrated by the proteins from hyperthermophilic *T. maritima*. Both 4Fe-4S ferredoxin (1VJW) and chemotaxis protein, CheY (1TMY), exhibit lower transition temperatures than their respective mesophilic counterparts (Figure 1D and E). Apparently the mechanism of thermal stability for ferredoxin and CheY protein from *T. maritima* may be different from those of other (hyper)thermostable proteins studied in our unfolding simulations. Do proteins from *T.maritima* follow an

alternative strategy to increase their thermostability? And if different strategies co-exist, what is the evolutionary basis for such different ways of thermal adaptation? First answers to these questions can be obtained from the analysis of the data presented in Table 1.

According to the data in Table 1, hydrolase from the thermophilic bacteria has lower total van der Waals energy compared to its mesophilic counterpart. There are 6  $\alpha$ -helices in thermophilic protein and only 3  $\alpha$ -helices in the mesophilic one. Elements of secondary structure in thermostable hydrolase (2PRD) are rather extended in size, comprising 105 residues versus 84 in the case of the mesophilic protein (1INO). The total number of hydrogen bonds is also higher in a protein from the thermophilic organism: 170 versus 145. Thus, according to all structural factors presented in Table 1 hydrolase from *T. thermophilus* is expected to be more stable compared to its mesophilic counterpart.

Another interesting feature of unfolding of hydrolases is almost complete coincidence of temperature-dependence curves of unfolding energies up to some relatively high temperature, followed by their abrupt separation. This can be explained by the difference in side-chain entropy of proteins due to the difference in their amino acid sequences.

Calculation of the average number of rotamers per residue in fully unfolded state (23) gives values 12.0 and 11.4 for the mesophilic and the thermophilic proteins, respectively.

It demonstrates, thus, higher side-chain entropy in the unfolded state of mesophilic hydrolase, which leads to its unfolding at lower temperature compared to thermophilic structure.

Hyperthermophilic rubredoxin from the archaebacteria *P. furiosus* demonstrates a pronounced bias towards high packing compared to mesophilic proteins (112 van der

Waals contacts per residue in hyperthermophilic protein compared to 103, 98, and 96 in the mesophilic analogues). Higher density of packing in hyperthermophilic proteins is also reflected in the increased number of H-bonds per residue and in the involvement of 62 per cent of residues into the elements of secondary structure compared to 39-40 per cent in mesophilic proteins.

Van der Waals interactions and involvement of more residues into elements of secondary structure contribute to an increase of stability of thermophilic 2Fe-2S ferredoxin (2CJN, H-bonds can not be obtained because of low resolution NMR structure), in agreement with the conclusion done in experimental work (24).

All major structural factors presented in Table 1 point out to increased thermostability in thermophilic 4Fe-4S ferredoxin (1IQZ) and, thus, explain its higher transition temperatures in unfolding simulations compared to mesophilic analogues.

Proteins from *T. maritima* show a principally different distribution of major stabilizing interactions (Table 1). Analysis of the data for 4Fe-4S ferredoxin (1VJW) gives a substantially increased number of hydrogen bonds and involvement of almost half of the residues into secondary structure elements. At the same time, compactness of the structure (95 van der Waals contacts per residue in hyperthermophilic proteins compared to 96 and 82 in two mesophilic proteins) is practically the same as those in mesophilic protein. CheY protein (1TMY) has a decreased number of van der Waals contacts and hydrogen bonds, and slightly higher fraction of residues participating in secondary structure. Thus, both unfolding simulations (Figure 1) and structural analysis (Table 1) demonstrate that increased stability of thermophilic hydrolase (1INO), ferredoxins (2CJN and 1IQZ), and hyperthermophilic rubredoxin (1CAA) from *P. furiosus* is provided by the

majority of structural factors acting together, whereas ferredoxin and CheY proteins from hyperthermophilic *T. maritima* lack structural connotation in their stabilizing mechanisms. This suggests that proteins from *T. maritima* have yet another way of increasing thermostability. In order to uncover a possible alternative mechanism of thermostability employed by *T. maritima* proteins we consider second major factor in protein stability, sequence.

We examined here sequence alignments of mesophilic proteins and their (hyper)thermophilic homologues (see Figure 2, which is published as supporting information on the PNAS web site). Results of quantitative analysis of sequence comparisons are presented in Table 2. Similarly to unfolding simulations, sequence analysis discriminates proteins from hyperthermostable *T. maritima* from other (hyper)thermostable proteins analyzed in this work. Their sequences demonstrate pronounced difference in the alignments with their mesophilic counterparts (see the explanation of definition of residues in the Legend to Table 2). They have lower sequence identity with mesophilic proteins than other (hyper)thermophilic proteins (40 and 33 percent, percentage of residue types I and II in Table 2 summed up together, and positions colored by light and dark gray in Figure 2) for ferredoxin and CheY protein, respectively. Moreover, 22 and 38 percent of sequence positions of *T. maritima* proteins do not match those in the sequences of mesophiles, while amino acids in the same positions of mesophilic sequences are identical to each other (light blue, Figure 2 of Supplementary material). In addition, we obtained substantial redistribution and increased number of charged residues in CheY protein and almost twice greater number of charged residues (11 versus 6, see also Table 2 and Figure 2) in ferredoxin, both from

*T. maritima*, contrasted to their mesophilic counterparts. High level of sequence variation compared to mesophilic orthologs and significant bias towards charged residues in their sequences point out to key role of sequence selection in adaptation of *T. maritima* proteins to extreme conditions of the environment, in contrast to other (hyper)thermophilic organisms such as *P. furiosus* and *T. thermophilus* where structural bias is more pronounced. Remarkably, this finding is completely supported by experimental data where decisive role of ion interactions in hyperthermostability of proteins from *T. maritima* was demonstrated (25, 26).

Among other proteins with increased stability analyzed in this work are thermophilic hydrolase (1INO), ferredoxins (2CJN and 1IQZ), and hyperthermophilic rubredoxin (1CAA). They exhibit high level of sequence identity (up to 80 percent) with their mesophilic orthologues (residue types I and II in Table 2; light and dark gray in Figure 2). Further, no significant substitutions into charged residues in sequences of respective (hyper)thermophiles were observed (positions marked by blue and red (Figure 2) and residue types IV and V in Table 2, respectively). Moreover, in the case of hyperthermophilic rubredoxin from *P. furiosus* (1CAA) and thermophilic ferredoxin from *S. elongatus* (2CJN) sequences of mesophiles contain in common parts of the alignments even more charged residues than their (hyper)thermophilic homologues (11 and 10 versus 4 and 3 per cent, respectively). Thus, all the approaches used in this work, structure-based unfolding simulations, analysis of structural features, and sequence alignments consistently distinguish proteins of *T. maritima* from the other (hyper)thermophilic proteins according to the differences in the ways of gaining thermostability. In the first case of thermophilic hydrolase (1INO), ferredoxins (2CJN and 1IQZ), and

hyperthermophilic rubredoxin (1CAA), we have a general trend of increasing of transition temperature obtained in unfolding simulations with a Go model, essentially structure-based approach. We also found, for these proteins, that all stabilizing structural factors act concurrently, which points to compactness as the most probable cause for *structure-based* original mechanism of higher stability.

In the second case of proteins from *T. maritima*, we did not observe structural connotation for the mechanism of thermostability. At the same time, we revealed a strong sequence bias in proteins from *T. maritima*, which demonstrated preference for some of the stabilizing interactions and not others: a mechanism that we define as *sequence-based* strategy.

While the differences between mechanisms of thermostability demonstrated in this study for several proteins are suggestive, a fully conclusive evidence can be obtained only from massive comparison of proteins from different species.

. Our previous analysis suggested dominance of structure-based strategy in hyperthermophilic archaea *P. furiosus* and in thermophilic bacteria *T. thermophilus*, but not in hyperthermophilic bacteria *T. maritima*. This defined a choice of the organisms to compare structural features of their proteomes, namely packing densities. To this end we compared distributions of van der Waals contacts in proteomes of different organisms. We analyzed distributions of van der Waals interactions in representative sets of major fold types (all  $\alpha$ , all  $\beta$ ,  $\alpha/\beta$ , and  $\alpha+\beta$ , see Table 3) from *T. maritima*, *P. furiosus/horikpshii/abissy*, and *T. thermophilus*. The data presented in Table 3 clearly demonstrates difference in the distribution of number of contacts per residue. Proteins from *Pyrococcus* and *T. thermophilus* have higher mean values compared to proteins

from *T.maritima* (275 and 272 contacts per residue versus 254, respectively). Besides, comparison of *T. maritima*, *Pyrococcus* and *T. thermophilus* proteins with those of mesophilic Yeast demonstrates that according to distributions of number of contacts *T. maritima* is closer to mesophilic organism rather than to *Pyrococcus* and *T. thermophilus* (data not shown). Kolmogorov-Smirnov (KS) test shows high statistical significance of the difference between the distributions of contacts of the compared sets (see Table 3). This further proves persistence of structure-based strategy in *T. thermophilus*, whereas in *T. maritima* we found transition to sequence-based mechanism.

The existence of the two mechanisms of thermostability, structure-based and sequence-based, gives us an opportunity to look at adaptation process from the perspective of general concepts, structure and sequence. Using this approach, we can determine which strategy has been utilized by nature in any particular case and to find possible ways of their alteration/modification. As an example we take ferredoxins, whose universal presence in all organisms makes them an outstanding object for our analysis. There is a special interest in the group of 2Fe-2S ferredoxins, the ferredoxin from the halophilic archaeobacterium *H. marismortui* (1DOI). First, this protein demonstrates a higher transition temperature (Figure 1) in unfolding simulations with structure-based Go potential, which can be explained by significantly increased packing density and extensive hydrogen bonding (Table 1). It is worth noting that this halophilic protein is from archaeobacteria, and it has substantially higher packing density than its mesophilic counterparts. This is another example (the first one is hyperthermophilic rubredoxin from archaeobacteria *P. furiosus*) which corroborates the idea of high packing density as one of ancient mechanisms of thermostability (15). At the same time one can easily trace way of

adaptation to high salinity. Almost entire surface of the protein is coated with acidic residues. This is achieved by enrichment of the sequence with acidic residues, in particular 8 of 22 residues in N-terminal domain are acidic, providing extra surface carboxylates for solvation. Thus, we observed co-existence of two stabilizing mechanisms: (i) specific, sequence-based, mainly by the abundance of acidic residues on the surface (27), which provides adaptation to high salinity, and (ii) non-specific, structure-based, which includes major factors of the protein stability and may well preserve stability and function of the protein under decreased salinity (27). This example highlights universality of two-strategy mechanism of adaptation, demonstrating versatility of adaptation to other than temperature factors of extreme environment. Finally, this example generalizes our finding of two-strategy mechanism to adaptation to wider spectrum of environmental conditions (temperature, salinity, pressure, etc.).

## **Discussion**

Earlier studies of the mechanisms of protein thermostability resulted in the discovery of a variety of contributors to the effect (1-5, 7-14, 28), and corresponding models on the basis of their combinations (4, 5). However, the diversity of the protein folds, the mechanisms of stability, and the evolutionary history of respective species raised questions about fundamental physical and evolutionary nature of organismic adaptation to high temperature and other extreme conditions (28). Here, we demonstrated how simple all-atom simulations can be used to estimate relative thermostability of the proteins from species with different growth temperature: mesophilic (growth temperature up to 60°C), thermophilic (up to 80°C), and hyperthermophilic (more than 80°C). By

analogy with microcalorimetric experiments (29), where the transition temperature of unfolding is used as one of the parameters to evaluate protein thermostability, we compared transition temperatures of unfolding obtained in simulations on the basis of the Go model (30). It was demonstrated (30) that Go-like models that consider only native interactions give a satisfactory description of two-state folding processes of single-domain proteins. We started from the assumption that for the same reasons, it adequately reflects stability of the structure during its unfolding (22), and our results justified the use of the Go model for discerning the cumulative effect of a variety of factors contributing to protein thermostability. Further, our analysis provides a new insight into physical mechanisms of thermostabilization showing two major strategies of increasing protein stability. The first strategy, structure-based, is achieved via selection of more compact structures so that relatively few changes in sequences are needed to achieve high thermal stability. We found structure-based stabilization for thermophilic hydrolase from *T. thermophilus*, 2Fe-2S ferredoxin from *S. elongatus*, and 4Fe-4S ferredoxin from *B. thermoproteolyticus*, and hyperthermophilic rubredoxin from *P. furiosus*, which feature more compact folds so that all stabilizing interactions contribute to enhanced thermostability (see Table I). We also found an alternative strategy of specific stabilization, where protein sequences are selected in such a way to enhance only one or few types of interactions in order to adapt to very specific extreme conditions. In this case, sequence variation, a mechanism that can introduce particular stabilizing interactions regardless of the detail of the original structure, gives rise to sequence-based specific strategy. Hyperthermophilic ferredoxin and chemotaxis protein from *T. maritima* exemplify this mechanism of stabilization. Here, the obvious bias towards specific

interactions couples with lack of non-specific structure-based stabilization. These results are corroborated by the experimental data, revealing that hyperthermostable ferredoxin at 25 °C is “thermodynamically not more stable than an average mesophilic protein” (31) and “conventional explanations for the structural basis of enhanced thermostability” do not work in case of chemotaxis protein from *T. maritima* (25). At the same time, stability of these proteins under extremely high temperatures is provided by significant modifications of their sequences towards enrichment by charged residues, which turned out to be an effective sequence-based method of adaptation to extreme specific conditions (31, 32).

Last but not least we discuss here what determines choice of a strategy during long-time evolutionary experiment. On the basis of our data we can point to two major determinants: environment and evolutionary potential (availability of different repertoires of sequences and structures as subjects for exploration at distinct stages of protein evolution). Selection of a specific strategy, then, is a direct result of a compromise between these two major groups of factors. First of all, proteins should develop effective mechanisms of thermostability or even combine it with adaptation to other specific factors (e.g. halophilic ferredoxin from *H. marismortui*). At the same time, the choice of the mechanism is determined by the current complexity of the structure and sequence repertoire available at a given stage of evolution and effectiveness of the existing mutation machinery. At the earliest stages, when proteins had rather restricted repertoire of sequences and only few effective mechanisms of adaptation, they used simple but robust mechanisms (working in a wide range of temperatures and independent of different physico-chemical conditions) by using structural potential of available folds and

developing, thus, structure-based mechanism of thermostability. Indeed, it was shown that thermophilic proteins have more designable folds (15), which can be adopted by greater numbers of sequences (33). Using more designable folds make it easier to find sequences with enhanced stability (15). In structural terms, designability correlates with the number of contacts per monomer, i.e. compactness (34, 35), and, thus, corroborates the choice of general strategy of thermostability in the beginning of protein evolution. Archaea proteins, rubredoxin from *P. furiosus* and 2Fe-2S ferredoxin from *H. marismortui*, exemplify a start from the ancient mechanism of stability, compactness (15). Later in evolution structure-based strategy can persist in some cases, while it can be replaced by more specific, sequence-based, strategy in other cases (related to diverse environmental conditions and distinct evolutionary path they underwent). High-throughput structural analysis of major fold types implemented in this work provided the evidence of persistence/changing strategy of stabilization. We obtained non-specific structure-based mechanism in proteins of ancient Archaea (here, *Pyrococcus*) and its persistence and substantiation in bacteria *T. thermophilus*. At the same time this strategy was abandoned in other bacteria, *T. maritima*, where sequence-based strategy of implementing specific interactions was eventually developed. The specificity and the difference in mechanisms of thermostability can reflect both long evolutionary distance between bacteria and representatives of Archaea kingdom and specific connection between some of them. This idea received strong support from the analysis of the complete genome of *T. maritima* (36) and phylogenetic consideration of its relationship to Archaea (37, 38). Earlier analysis revealed that by means of whole-genome similarity comparison, *T. maritima* has 24 per cent of genes that are most similar to Archaea's.

High level of similarity is a consequence of lateral (or horizontal) gene transfer (36, 39), which, as it was demonstrated earlier, points to specific biochemical and environmental adaptations (40-43). Thus, when *T. maritima* invaded the hot environment, it developed mechanisms of thermostability in order to reach adaptation. At the same time, this environment was already colonized by Archaea which served eventually as a source for lateral gene transfer. Lateral gene transfer demonstrates organismal level of adaptation during recolonization (36), consistent with the long evolutionary distance between *T. maritima* and Archaea. This observation reveals a new, interesting phenomenon: distinctions in sequences/structures and molecular/cellular machinery at different stages of evolution can play decisive role in addition to the environmental conditions. Finally, traces of ancient mechanisms of thermostability in proteins from archaeobacteria and ways of adaptation of proteins from *T. maritima* leads us to the self-consistent model of two-strategy choice for thermostability at different stages of evolution: (i) the simplest and most reliable *non-specific* structure-based mechanism of thermostability at the very beginning of life under hot conditions, which started from the ancient structural implement, compactness, and in absence of developed molecular/cellular machinery; (ii) sequence-based specific adaptation to hot conditions at later stages of protein evolution (*e.g.* recolonization), by utilizing whole spectrum of structural and genomic opportunities developed to date in diversity of species.

The two-strategy model of protein thermostability provides a coherent viewpoint into interplay of physical and evolutionary factors that give rise to protein thermostability in the context of organismal adaptation. Potentially it can be helpful in guiding our effort to design proteins with desired thermal properties..

## **Acknowledgements**

The authors thank Jun Shimada for help with the unfolding simulations, Brian Dominy for the helpful discussions. Critical reading and valuable comments by William Chen and Emmanuel Tannenbaum are greatly appreciated. This work is supported by NIH RO1 52126

## References

1. Elcock, A. H. (1998) *J Mol Biol* 284, 489-502.
2. Vogt, G., Woell, S. & Argos, P. (1997) *J Mol Biol* 269, 631-43.
3. Szilagyi, A. & Zavodszky, P. (2000) *Structure Fold Des* 8, 493-504.
4. Jaenicke, R. (1991) *Eur J Biochem* 202, 715-28.
5. Jaenicke, R. & Bohm, G. (1998) *Curr Opin Struct Biol* 8, 738-48.
6. Makhatadze, G. I. & Privalov, P. L. (1995) *Adv Protein Chem* 47, 307-425.
7. Jaenicke, R. (1999) *Prog Biophys Mol Biol* 71, 155-241.
8. Berezovsky, I. N., Tumanyan, V. G. & Esipova, N. G. (1997) *FEBS Lett* 418, 43-6.
9. Schumann, J., Bohm, G., Schumacher, G., Rudolph, R. & Jaenicke, R. (1993) *Protein Sci* 2, 1612-20.
10. Querol, E., Perez-Pons, J. A. & Mozo-Villarias, A. (1996) *Protein Eng* 9, 265-71.
11. Vetriani, C., Maeder, D. L., Tolliday, N., Yip, K. S., Stillman, T. J., Britton, K. L., Rice, D. W., Klump, H. H. & Robb, F. T. (1998) *Proc Natl Acad Sci U S A* 95, 12300-5.
12. Hurley, J. H., Baase, W. A. & Matthews, B. W. (1992) *J Mol Biol* 224, 1143-59.
13. Thompson, M. J. & Eisenberg, D. (1999) *J Mol Biol* 290, 595-604.
14. Jaenicke, R. (2000) *Proc Natl Acad Sci U S A* 97, 2962-4.
15. England, J. L., Shakhnovich, B. E. & Shakhnovich, E. I. (2003) *Proc Natl Acad Sci U S A* 100, 8727-31.
16. Berezovsky, I. N., Namiot, V. A., Tumanyan, V. G. & Esipova, N. G. (1999) *J Biomol Struct Dyn* 17, 133-55.
17. Shimada, J., Kussell, E. L. & Shakhnovich, E. I. (2001) *J Mol Biol* 308, 79-95.
18. Murzin, A. G., Brenner, S. E., Hubbard, T. & Chothia, C. (1995) *J Mol Biol* 247, 536-40.
19. Stickle, D. F., Presta, L. G., Dill, K. A. & Rose, G. D. (1992) *J Mol Biol* 226, 1143-59.
20. Berezovskii, I. N., Esipova, N. G. & Tumanian, V. G. (1998) *Biofizika* 43, 392-402.
21. Corpet, F. (1988) *Nucleic Acids Res* 16, 10881-90.
22. Go, N. & Abe, H. (1981) *Biopolymers* 20, 991-1011.
23. Canutescu, A. A., Shelenkov, A. A. & Dunbrack, R. L., Jr. (2003) *Protein Sci* 12, 2001-14.
24. Hatanaka, H., Tanimura, R., Katoh, S. & Inagaki, F. (1997) *J Mol Biol* 268, 922-33.
25. Usher, K. C., de la Cruz, A. F., Dahlquist, F. W., Swanson, R. V., Simon, M. I. & Remington, S. J. (1998) *Protein Sci* 7, 403-12.
26. Macedo-Ribeiro, S., Darimont, B., Sterner, R. & Huber, R. (1996) *Structure* 4, 1291-301.
27. Frolow, F., Harel, M., Sussman, J. L., Mevarech, M. & Shoham, M. (1996) *Nat Struct Biol* 3, 452-8.
28. Jaenicke, R. (2000) *J Biotechnol* 79, 193-203.
29. Privalov, G. P. & Privalov, P. L. (2000) *Methods Enzymol* 323, 31-62.
30. Go, N. (1983) *Annu Rev Biophys Bioeng* 12, 183-210.
31. Pfeil, W., Gesierich, U., Kleemann, G. R. & Sterner, R. (1997) *J Mol Biol* 272, 591-6.
32. Torrez, M., Schultehenrich, M. & Livesay, D. R. (2003) *Biophys J* 85, 2845-53.
33. Li, H., Helling, R., Tang, C. & Wingreen, N. (1996) *Science* 273, 666-9.
34. Wolynes, P. G. (1996) *Proc Natl Acad Sci U S A* 93, 14249-55.
35. Shakhnovich, E. I. (1998) *Fold Des* 3, R45-58.
36. Nelson, K. E., Clayton, R. A., Gill, S. R., Gwinn, M. L., Dodson, R. J., Haft, D. H., Hickey, E. K., Peterson, J. D., Nelson, W. C., Ketchum, K. A., et al. (1999) *Nature* 399, 323-9.
37. Nesbo, C. L., L'Haridon, S., Stetter, K. O. & Doolittle, W. F. (2001) *Mol Biol Evol* 18, 362-75.
38. Daubin, V., Gouy, M. & Perriere, G. (2001) *Genome Inform Ser Workshop Genome Inform* 12, 155-64.
39. Lawrence, J. G. & Ochman, H. (1997) *J Mol Evol* 44, 383-97.
40. Doolittle, W. F. (1999) *Trends Cell Biol* 9, M5-8.
41. Doolittle, W. F. (1999) *Science* 284, 2124-9.
42. Jain, R., Rivera, M. C. & Lake, J. A. (1999) *Proc Natl Acad Sci U S A* 96, 3801-6.
43. Lawrence, J. G. (1999) *Curr Opin Microbiol* 2, 519-23.

## Figure legends

**Figure 1.** The temperature-dependence of the energy of unfolding. Every simulation of unfolding started from the native structure and included  $2 \cdot 10^6$  MC steps. Absolute temperature increment is 0.2, and 0.1 in the vicinity of transition temperature. In all plots curves of the unfolding energy of mesophilic proteins are shown by black, blue, or cyan dots; thermophilic proteins – red dots; hyperthermophilic proteins – orange dots; halophilic protein – green dots. **A.** Hydrolases, from *E.coli* (1INO, black rhombuses) and *T. thermophilus* (2PRD, red squares); **B.** Rubredoxins, from *D. gigas* (1RDG, cyan triangulares), *C. pasteurianum* (5RXN, black rhombuses), *D. vulgaris* (8RXN, blue rhombuses), and *P. furiosus* (1CAA, orange squares). **C.** 2Fe-2S Ferredoxin, from *S. platensis* (4FXC, cyan triangulares), *E. arvensis* (1FRR, black rhombuses), *Anabaena PCC7120* (1FRD, blue rhombuses), *H. marismortui* (1DOI, green rhombuses), and *S. elongatus* (2CJN, red squares); **D.** 4Fe-4S Ferredoxin, from *C. acidi-urici* (1FCA, black triangulares), *P. asaccharolyticus* (1DUR, blue rhombuses), *B. thermoproteolyticus* (1IQZ, red squares), and *T. maritima* (1VJW, orange squares); **E.** Chemotaxis protein, from *E. coli* (3CHY, blue rhombuses), *S. typhimurium* (2CHF, black squares), and *T. maritima* (1TMY, orange squares).

## Legends to Tables

**Table 1.** Factors possibly contributing of thermostability of analyzed proteins. Van der Waals interactions (16), number of H-bonds (19, 20) and amount of residues involved into elements of secondary structure in groups of proteins under consideration.

Parameters in the Table are as follows: vdW conts – total number of vdW contacts in protein; Cnts/res – number of vdW contacts per residue; N of bonds – number of H-bonds in protein; Bnds/res – number of H-bonds per residue; Sec. Strct – percentage of residues involved into the elements of secondary structure. Names of (hyper)thermophilic organisms in column 2 are bolded italic.

**Table 2.** Quantitative results of the examination of sequence alignments for the groups of analyzed proteins (Column 1). Only common parts of the alignments (see Figure 2 of Supporting information) are considered for calculation of Table 2. Types of residues are defined as follows: Type 1 (light gray in Figure 2 - residue in the sequence of the (hyper)thermophile is identical to at least one of those in respective position of mesophilic sequences; Type 2 (dark gray, Figure 2) – presence of charged residues in respective positions of (hyper)thermophilic and at least one of the mesophilic sequences; Type 3 (light blue, Figure 2) – identical non-charged residues in respective positions of at least two mesophilic sequences, while non-matching residue in (hyper)thermophile; Type 4 (blue, Figure 2) – charged residue in at least one of the mesophiles, but non-charged residues in (hyper)thermophile; Type 5 (red, Figure 2) – charged residues in the (hyper)thermophile, while non-charged residues in respective positions of mesophilic proteins.

**Table 3.** Comparative analyzes of the distributions of van der Waals contacts in representatives of the major fold types from *P. abyssi/horikoshii/furiosus*, *T. maritima*, and *T. thermophilus* (for the listing of the analyzed PDB structures see supporting information which is published on the PNAS web site). Kolmogorov-Smirnov test have been applied to united sets of the folds presented in each source. Results of the test are presented in a third column: number in brackets is P-value; *Tm* and *Tt* are *T. maritima* and *T. thermophilus*, respectively, and demonstrate differences between their proteins and those from the source (column 1). Last column (Fold types) demonstrates mean values of the distributions for major fold types in proteins from the respective organisms.

**Table 1**

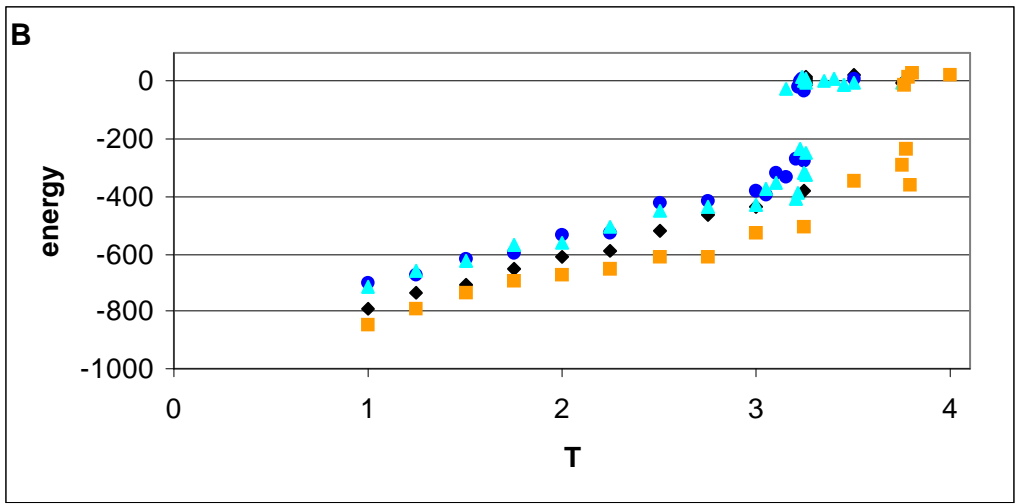
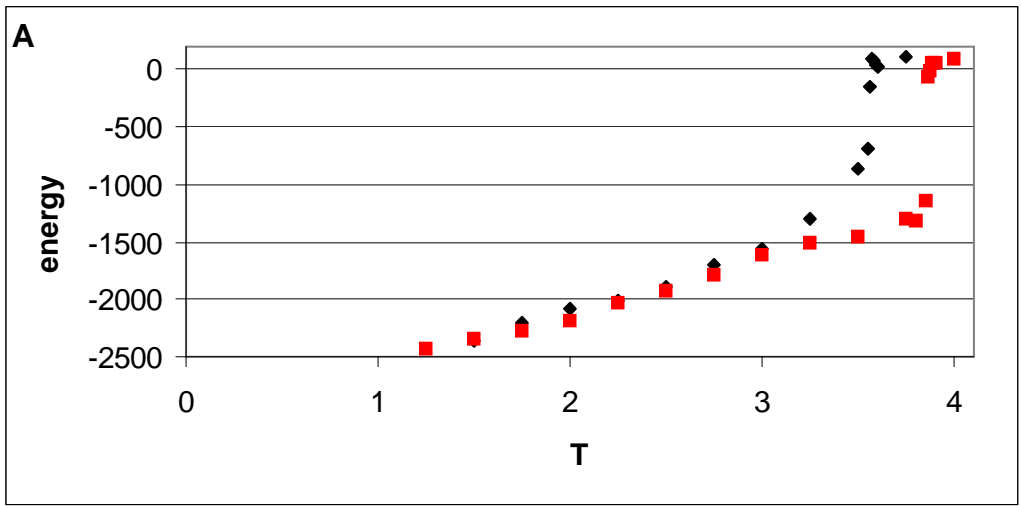
Protein	Source	VdW energy		Hydrogen bonds		Sec. Strct
		vdW conts	Cnts /res	N of bnds	Bnds /res	
<b>Hydrolase</b>						
1INO (175)	<i>E. coli</i>	22804	130	145	0.83	0.48
2PRD(174)	<i>T. thermophilus</i>	23178	133	170	0.98	0.6
<b>Rubredoxin</b>						
1RDG (52)	<i>D. gigas</i>	5363	103	40	0.77	0.40
5RXN (54)	<i>C. pasteurianum</i>	5296	98	39	0.72	0.39
8RXN (55)	<i>D. vulgaris</i>	5292	96	42	0.76	0.4
1CAA (53)	<i>P. furiosus</i>	5914	112	45	0.85	0.62
<b>Ferredoxin (2FE-2S)</b>						
4FXC (98)	<i>S. platensis</i>	11005	113	76	0.78	0.37
1FRR (95)	<i>E. arvense</i>	11767	124	96	1.01	0.43
1FRD (98)	<i>Anabaena PCC7120</i>	12032	123	102	1.04	0.49
1DOI (128)	<i>H. marismortui</i>	17537	137	131	1.02	0.5
2CJN (97)	<i>S. elongatus</i>	13429	138	-	-	0.56
<b>Ferredoxin (4FE-4S)</b>						
1FCA (55)	<i>C. acidurici</i>	5293	96	39	0.71	0.22
1DUR (55)	<i>P. asaccharolyticus</i>	4507	82	37	0.67	0.4
1IQZ (81)	<i>B. thermoproteolyticus</i>	9152	113	74	0.90	0.44
1VJW (59)	<i>T. maritima</i>	5591	95	57	0.97	0.49
<b>Chemotaxis Protein</b>						
3CHY (128)	<i>E. coli</i>	17263	135	164	1.28	0.58
2CHF (128)	<i>S. typhimurium</i>	17361	136	166	1.3	0.58
1TMY (118)	<i>T. maritima</i>	15507	131	134	1.14	0.7

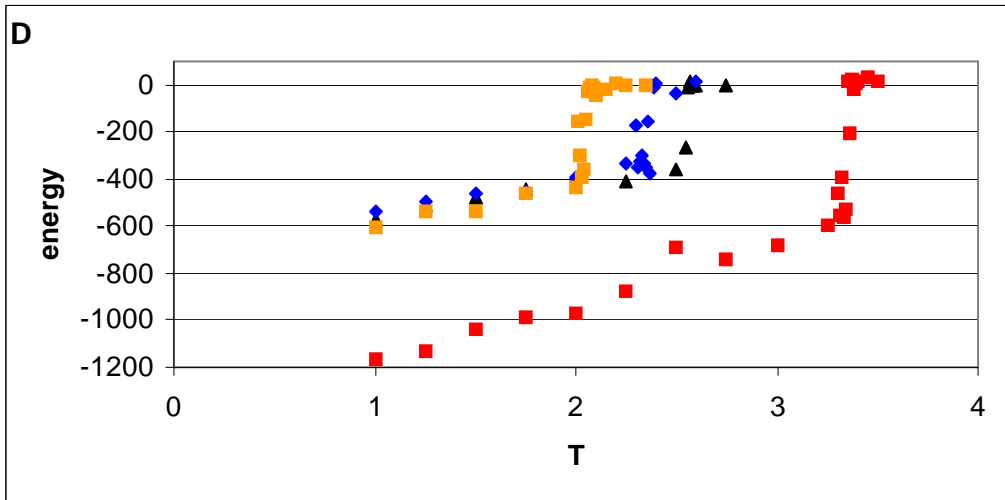
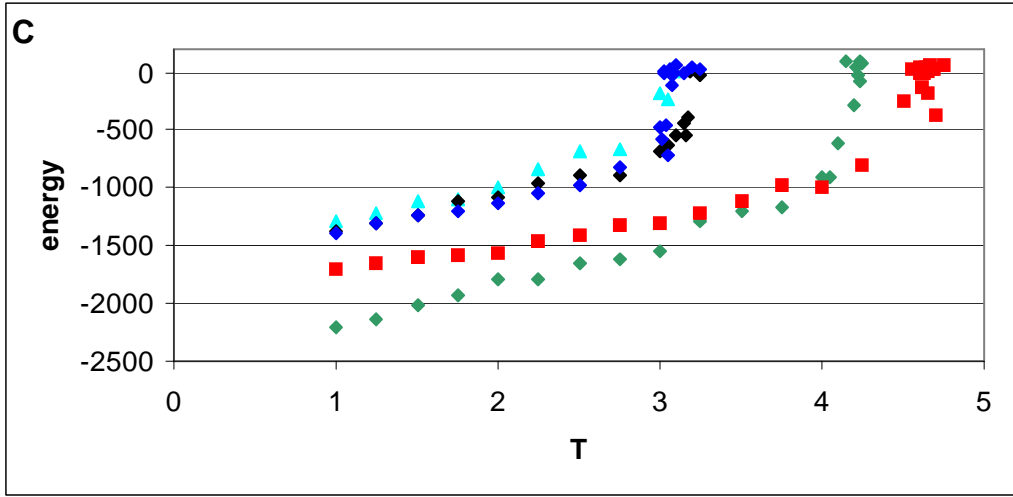
**Table 2**

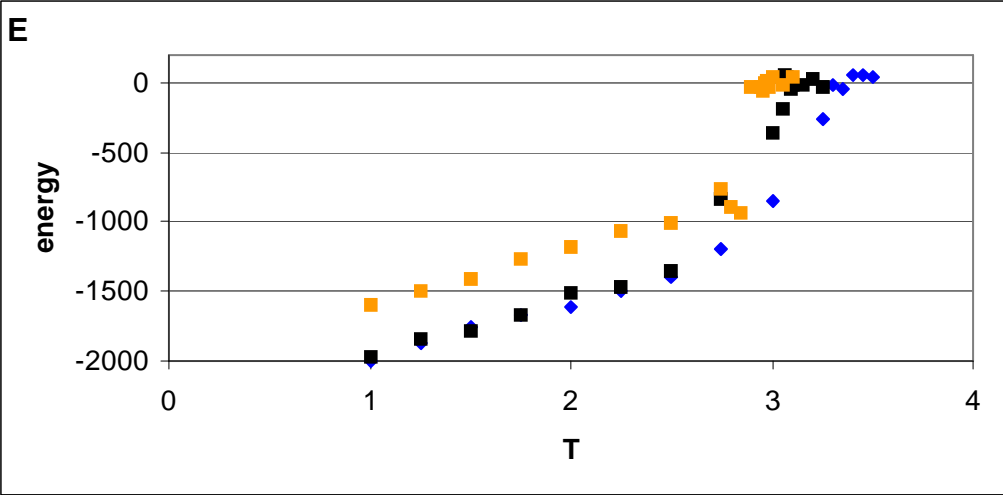
Proteins under comparison	Size of the common part of the alignments	Number of residues (percentage)				
		Type 1	Type 2	Type 3	Type 4	Type 5
<b>1INO versus 2PRD</b>	178	52 (29)	38 (21)	-	16 (9)	16 (9)
<b>1RDG/5RXN/8RXN versus 1CAA</b>	54	24 (44)	17 (32)	4 (7)	6 (11)	2 (4)
<b>1FCA/1DUR versus 1IQZ</b>	58	15 (26)	6 (10)	15 (26)	6 (10)	10 (17)
<b>1FRD/4FXC/1FRR versus 2CJN</b>	99	53 (54)	26 (26)	5 (5)	10 (10)	3 (3)
<b>1FRD/4FXC/1FRR versus 1DOI</b>	99	30 (30)	22 (22)	22 (22)	14 (14)	9 (9)
<b>1FCA/1DUR versus 1VJW</b>	60	18 (30)	6 (10)	13 (22)	6 (10)	11 (18)
<b>3CHY/2CHF versus 1TMY</b>	124	24 (19)	16 (14)	47 (38)	16 (14)	19 (15)

**Table 3**

Source	Total number of folds or proteins /domains	Mean value of the distribution of number of vdW contacts per residue and KS-test (p-values)	Fold types			
			All $\alpha$	All $\beta$	$\alpha/\beta$	$\alpha+\beta$
<i>P. abyssi/furiosus/horikoshii</i>	37	275 $T_m$ ( $7.68 \cdot 10^{-2}$ ) $T_t$ ( $2.6 \cdot 10^{-2}$ )	282	238	284	296
<i>T. maritima</i>	42	254 $T_t$ ( $1.7 \cdot 10^{-1}$ )	269	236	265	233
<i>T. thermophilus</i>	38	272	273	269	276	-







## Supporting information.

**Legend to Figure 2.** Sequence alignments for the groups of analyzed proteins. Only common parts of the alignments are presented and considered for calculation of Table 2. Letters are coloured as follows: light gray – the residue in the sequence of the (hyper)thermophile is identical to at least one of those in respective position of mesophilic sequences; dark gray – presence of charged residues in respective positions of (hyper)thermophilic and at least one of the mesophilic sequences; light blue – identical non-charged residues in respective positions of at least two mesophilic sequences, while non-matching residue in (hyper)thermophile; blue – charged residue in at least one of the mesophiles, but non-charged residues in (hyper)thermophile; red – charged residues in the (hyper)thermophile, while non-charged residues in respective positions of mesophilic proteins. **A.** Hydrolases: 1ino(*Ec*) versus 2prd(*Tt*); **B.** Rubredoxins: 1rdg(*Dg*)/5rxn(*Cp*)/8rxn(*Dv*) versus 1caa(*Pf*); **C.** 4Fe-4S Ferredoxins: 1FCA(*Ca*)/1DUR(*Pa*) versus 1IQZ(*Bt*); **D.** 2Fe-2S Ferredoxins: 1FRD(*Anabaena*)/4FXC(*Sp*)/1FRR(*Ea*) versus 2CJN (*Se*); **E.** 2Fe-2S Ferredoxins: 1FRD(*Anabaena*)/4FXC(*Sp*)/1FRR(*Ea*) versus 1DOI(*Hm*); **F.** 4Fe-4S Ferredoxins: 1FCA(*Ca*)/1DUR(*Pa*) versus 1VJW(*Tm*); **G.** Chemotaxis proteins: 3CHY(*Ec*)/2CHF(*St*) versus 1TMY(*Tm*).

## Figure 2

### A.

1ino: SLLNVPAGKDLPE<sup>D</sup>IYVVI<sup>E</sup>IIPANA<sup>D</sup>PIKYEID<sup>K</sup>ESGALFVDRFMSTAMFYPCNYGYIN<sup>H</sup>  
2prd: ANL<sup>K</sup>SLPVGDKAPEV<sup>V</sup>HMVIEV<sup>P</sup>R<sup>G</sup>SGN-KYEYD<sup>P</sup>DLGAI<sup>K</sup>LDRVLPGAQFY<sup>P</sup>G<sup>D</sup>YGFIPS

1ino: TLSLDGDPVDVLVPTPYPLQPGSVIRCRPVGVL<sup>K</sup>MTDEAGE<sup>D</sup>AKLVAVP<sup>H</sup>SKLS<sup>K</sup>KEYDHI  
2prd: TLA<sup>E</sup>DGDPLDGLVLSTYPLLPGVV<sup>E</sup>VRVVG<sup>L</sup>LLME<sup>D</sup>E<sup>K</sup>GGDAKVIGVVA<sup>E</sup>--D<sup>Q</sup>RLDHI

1ino: <sup>K</sup>DVNDLPELLKAQIAHFFEHY<sup>K</sup>DLE--KGK<sup>W</sup>V<sup>V</sup>E<sup>G</sup>WENAEAA<sup>K</sup>AEIVASF<sup>E</sup>RA<sup>K</sup>N<sup>K</sup>  
2prd: QDIGDVPEGV<sup>K</sup>Q<sup>E</sup>IQHFFETYKALE<sup>A</sup><sup>K</sup>KGK<sup>W</sup>V<sup>V</sup>TGWR<sup>D</sup>RKAAL<sup>E</sup>EV<sup>R</sup>ACIARY<sup>K</sup>G

### B.

1rdg: MDIYVCTVCGY<sup>E</sup>YDPAKGD<sup>P</sup>DSG<sup>I</sup>KPGTKFEDLPDDWACPVC<sup>G</sup>ASKDAFE<sup>K</sup>Q  
5rxn: MKKYTCTVCGY<sup>I</sup>YDPE<sup>D</sup>GD<sup>P</sup>DD<sup>G</sup>VNPGTDFKDI<sup>P</sup>DDWVCPLCGV<sup>G</sup>KDEFEE<sup>V</sup>EE  
8rxn: MKKYVCTVCGY<sup>E</sup>YDPA<sup>E</sup>EGD<sup>P</sup>DNGV<sup>K</sup>PGTSFDDLPA<sup>D</sup>WVCPVC<sup>G</sup>APKSEFE<sup>A</sup>A  
1caa: AK<sup>W</sup>V<sup>K</sup>ICGY<sup>I</sup>YD<sup>E</sup>DAGD<sup>P</sup>DNG<sup>I</sup>SPG<sup>T</sup>KFEELPDDWVCPIC<sup>G</sup>APKSEFE<sup>K</sup>LE<sup>D</sup>

### C.

1fca: <sup>A</sup>YVINEACISCGACE<sup>P</sup>EC<sup>P</sup>-V<sup>D</sup>AISQGSRY<sup>V</sup>ID-----<sup>A</sup>DT<sup>C</sup>IDCGACA-G  
1dur: <sup>A</sup>YVINDSCIACGACK<sup>P</sup>EC<sup>P</sup>-V<sup>N</sup>CI-QEGSIY<sup>A</sup>ID-----<sup>A</sup>D<sup>S</sup>CIDCGSCA-S  
1iqz: TIV<sup>D</sup>KETCIACGACGAAAP<sup>D</sup>IY<sup>D</sup>Y<sup>D</sup>ED<sup>E</sup>DGIAYVTL\*\*\*\*\*<sup>P</sup>DILID<sup>D</sup>MMDA<sup>F</sup>E

1fca: <sup>V</sup>CPVDAPVQA  
1dur: <sup>V</sup>CPVGAPNP<sup>E</sup>D  
1iqz: GCPTDSI<sup>K</sup>VAD

### D.

1frd: ASYQVRLINK<sup>K</sup>Q<sup>D</sup>IDTTIEI<sup>D</sup>EETTILDGAEENGI<sup>E</sup>LPFSCHSGSCSSCVG<sup>K</sup>VVEGEVDQ  
4fxc: ATYKVTLINEA<sup>E</sup>GIN<sup>E</sup>TIDCDD<sup>D</sup>TYILD<sup>A</sup>EEA<sup>G</sup>LDPYSCRAGACSTCAGTITSGTIDQ  
1frr: AYK<sup>T</sup>VLK<sup>T</sup>PSGEFTLDVPE<sup>G</sup>TTILD<sup>A</sup>EEA<sup>G</sup>YDLPFSCRAGACSSCLG<sup>K</sup>VVSGSVD<sup>E</sup>  
2cjn: ATYKVTLV<sup>R</sup>P-DGSETTIDVPE<sup>E</sup>YILDVAEEQGLDLPFSCRAGACSTCAGK<sup>L</sup>LEGEVDQ

1frd: SDQIFLDDEQMG-KGFALLCVTYPRSNCTIK<sup>T</sup>HQ<sup>E</sup>EPYLA  
4fxc: SDQSFLDDDQIE-AGYVLT<sup>C</sup>VAYPTSDCTIK<sup>T</sup>HQ<sup>E</sup>EGLY  
1frr: SEG<sup>S</sup>FLDDGQME-EGFVLT<sup>C</sup>IAIPESDLVI<sup>E</sup>TH<sup>K</sup>EEELF  
2cjn: SDQSFLDDDQIE-KGFVLT<sup>C</sup>VAYPRSD<sup>K</sup>ILT<sup>N</sup>Q<sup>E</sup>EELY

**E.**

1frd: ASYQVRLINKKQDIDTTIEIDEETTILDGAEENGIELPFSCHSGSCSSCVGKVVVEGEVDQ  
 4fxc: ATYKVTLINEAEGINETIDCDDDTYILDAAEEAGLDLPYSCRAGACSTCAGTITSGTIDQ  
 1frr: AYKTVLKTSPSGEFTLDVPEGTTILDAAEEAGYDLPFSCRAGACSSCLGKVVVSGSVDE  
 1doi: VFGEASDMDLDEDDYGSLEVNEG EYILEAAEAQGYDWPFSCRAGACANCAAIIVLEGDIDM

1frd: SDQIFLDDEQMG-KGFALLCVTYPRSNCTIKTHQEPYLA  
 4fxc: SDQSFLDDDQIE-AGYVLTCAVAYPTSDCTIKTHQEEGLY  
 1frr: SEGSFLDDGQME-EGFVLTCAIIPESDLVIETHKEEELF  
 1doi: SDMQQILDEEVEDKKNVRLTCIGSPDADEVKIVYNAKHL

**F.**

1fca: AYVINEACISCGACEPECP-VDAISQGGSRVIDADTCIDCGA-CAGVCPVDAPVQA  
 1dur: AYVINDSCIACGACKPECP-VNCI-QEGSIYAIADASCIDCGS-CASVCPVGAPNPED  
 1vjw: MKVRVDADACIGCVENLCPDVFQLGDDGKAKVLQPETDLPCAADAASCPTGAISVEE

**G.**

3chy: ADKELKFLVDDFSTMRRIVRNLLKELGFNNVEEAEDGVDALNKLQAGGYGFVISDNMP  
 2chf: ADKELKFLVDDFSTMRRIVRNLLKELGFNNVEEAEDGVDALNKLQAGGFIIISDNMP  
 1tmy: MGKRVLIIVDDAAFMRMMLKDIITKAGYEVAGEATNGREAVEKYKELKPDIVTMDITMP

3chy: NMDGLELLKTIIRADGAMSALPVLMTAEAKKENI IAAAQAGASGYVVKPFTAATLEEKLN  
 2chf: NMDGLELLKTIIRADSAMSALPVLMTAEAKKENI IAAAQAGASGYVVKPFTAATLEEKLN  
 1tmy: EMNGIDAIKEIMKIDPNAK--IIVCSAMGQQAMVIEAIKAGAKDFIVKPFQPSRVVEALN

3chy: KIFE  
 2chf: KIFE  
 1tmy: KVSK

**Listing of the PDB-codes for major fold types in *P. abyssi/horikoshii/furiosus*, *T. maritima*, and *T. thermophilus*. Total numbers of analyzed folds from *P. abyssi/horikoshii/furiosus*, *T. maritima*, and *T. thermophilus* are 37, 42, and 38, respectively. Numbers in the brackets show location of the fold in the structure.**

***P. abyssi/horikoshii/furiosus* folds:**

All alpha:

1AIS\_B(1108-1300),1AJ8,1AOR(211-605),1B43(220-339),1I1G(2-61),1IQP(89-169);

All beta:

1B8A(1-103),1DQ3\_1(1-128),1DQ3\_2(415-454),1DQI,1ELT,1H64,1IQ8\_1(506-582),1IZ6(2-70),1MXG(362-435),1PLZ;

Alpha/beta:

1A1S(1-150),1A8L(1-119),1E19,1G2I,1GDE,1GEF,  
1GTM(181-419),1HG3,1IM5,1IOF,1ION,1IQ8\_2,1J08,1JFL,1JG1,1LK5\_1(1-130),1LK5\_2(211-229);

Alpha plus beta:

1AIS\_A(1-92),1II7,1K9X,1NNW.

***T. maritima* folds:**

All alpha:

1J5Y(3-67),1JIO,1M6Y\_1(115-215),1O0W(1-167),1P2F\_1(121-217),1QC7;

All beta:

1GJW\_2(573-636),1GUI,1HH2(127-198),1I8A,1L1J,1NCJ(2-101),1O12\_1(1-43),  
1O12\_2(332-364),1O4T;

Alpha/beta:

1A5Z(22-163),1B9B,1D1G,1HDG,1I4N,1J9L,1JCF(1-140),1JG8,1L9G,1M6Y\_2(2-114),  
1M6Y\_3(216-294),1O0U,1O14,1O1X,1O20,1TMY,1VPE;

Alpha plus beta:

1DD5,1GXJ,1I58,1J6R,1M4Y,1NZ0,1O0X,1O22,1O26,1VJW;

***T. thermophilus* folds:**

All alpha:

1A8H(349-500),1B7Y\_B1(1-38),1C52,1DK1,1EE8(122-210),1GAX\_1(797-862),  
1GAX\_2(579-796),1IOM,1IQR\_1(172-416),1IW7\_E,1N97,1SES(1-110);

All beta:

1EHK\_B(41-168),1EXM\_1(213-312),1EXM\_2(313-405),1FEU,1GAX\_3(190-342),

1IZ0\_1(1-98),1KWG(591-644),1NYK,2CUA,2PRD;

Alpha/beta:

1BXB,1EXM\_3(3-212),1GAX\_4(1-189),1GAX\_5(343-578),1IQR\_2(2-171),1IR6,1IUK,1J09(1-305),1J33,1J3B,1J3N,1JL2,1KA9\_H,1ODK,1SRV,1XAA;